OECD/MCCI-2002-TR03

OECD MCCI Project
Melt Eruption Test (MET)
Design Report

Rev. 2 April 15, 2003

by:

M. T. Farmer, S. Lomperski, D. J. Kilsdonk, and R. W. Aeschlimann
Reactor Analysis and Engineering Division
Argonne National Laboratory
9700 S. Cass Avenue
Argonne, IL 60439 USA

S. Basu
Project Manager
U.S. Nuclear Regulatory Commission

TABLE OF CONTENTS

LIST OF FIGURES

LIST OF TABLES

1.0 INTRODUCTION

1.1 Background

The Melt Attack and Coolability Experiments (MACE) program at Argonne National Laboratory addressed the issue of the ability of water to cool and thermally stabilize a molten core-concrete interaction when the reactants are flooded from above. These tests provided data regarding the nature of corium interactions with concrete, the heat transfer rates from the melt to the overlying water pool, and the role of noncondensable gases in the mixing processes that contribute to melt quenching. The Melt Coolability and Concrete Interaction (MCCI) program is pursuing separate effect tests to examine the viability of the melt coolability mechanisms identified as part of the MACE program. These mechanisms include bulk cooling, water ingression, volcanic eruptions, and crust breach.

At the second PRG meeting held at ANL on 22-23 October 2002, a preliminary design[1] for a separate effects test to investigate the melt eruption cooling mechanism was presented for PRG review. At this meeting, NUPEC made several recommendations on the experiment approach aimed at optimizing the chances of achieving a floating crust boundary condition in this test. The principal recommendation was to incorporate a mortar sidewall liner into the test design, since data from the COTELS experiment program indicates that corium does not form a strong mechanical bond with this material. Other recommendations included: i) reduction of the electrode elevation to well below the melt upper surface elevation (since the crust may bond to these solid surfaces), and ii) favorably taper the mortar liner to facilitate crust detachment and relocation during the experiment. Finally, as a precursor to implementing these modifications, the PRG recommended the development of a design for a small-scale scoping test intended to verify the ability of the mortar liner to preclude formation of an anchored bridge crust under core-concrete interaction conditions. This revised Melt Eruption Test (MET) plan is intended to satisfy these PRG recommendations. Specifically, the revised plan focuses on providing data on the extent of crust growth and melt eruptions as a function of gas sparging rate under well-controlled experiment conditions, including a floating crust boundary condition.

1.2 Objectives

The overall objective of MET is to determine to what extent core debris is rendered coolable by eruptive-type processes that breach the crust *that rests upon* the melt. The specific objectives of this test are as follows:

- Evaluate the augmentation in surface heat flux during periods of melt eruption.

- Evaluate the melt entrainment coefficient from the heat flux and gas flow rate data for input into models that calculate ex-vessel debris coolability.

- Characterize the morphology and coolability of debris resulting from eruptive processes that transport melt into overlying water.

- Discriminate between periods when eruptions take the form of particle ejections into overlying water, leading to a porous particle bed, and single-phase extrusions, which lead to volcano-type structures.

1.3 Approach/Rationale

The experiment approach addresses the melt eruption cooling mechanism through a dedicated separate-effects experiment conducted with an inert basemat and gas sparging to simulate concrete decomposition gases. The use of an inert basemat eliminates the tendency of the melt to separate from the crust by the mechanism of basemat densification upon melting. The test design has been modified to incorporate a favorably tapered mortar sidewall liner and shortened tungsten electrodes (to remove solid surfaces upon which the crust may bond) to optimize the chances that the crust will slump downwards and maintain contact with the melt upper surface. The principal parameter influencing melt entrainment is the flow rate of decomposition gases. The use of an externally supplied gas source provides control over this critical parameter. Moreover, the flow rate (as opposed to the input power) can be used to increase the melt pool void fraction and reestablish melt/crust contact if separation were to occur. These steps circumvent shortcomings that were identified in MACE integral effects tests insofar as maintaining melt/crust contact.

The report begins by presenting the MET design that has been modified in accordance with the PRG recommendations. This design description is followed by presentation of a proposed test operating procedure. Finally, a design is proposed for a small-scale scoping test intended to verify the ability of the mortar liner to preclude formation of an anchored bridge crust under core-concrete interaction conditions.

2.0 EXPERIMENT DESCRIPTION

2.1 Test Apparatus

The overall MET system design is shown in Figure 2.1. The system consists of a test section, a power supply for direct electrical heating (DEH) of the melt, a water supply system, a quench system, and an offgas system. The overall design is identical to that used in previous MACE integral-effects tests[2], with the following exceptions:

i) the test section concrete basemat has been replaced with a porous MgO basemat with gas sparging to mock up concrete decomposition gases,

ii) a mortar sidewall liner is incorporated into the test section design, and

iii) the mass spectrometer has been omitted from the off gas system since concrete decomposition gases are not generated during the course of this test.

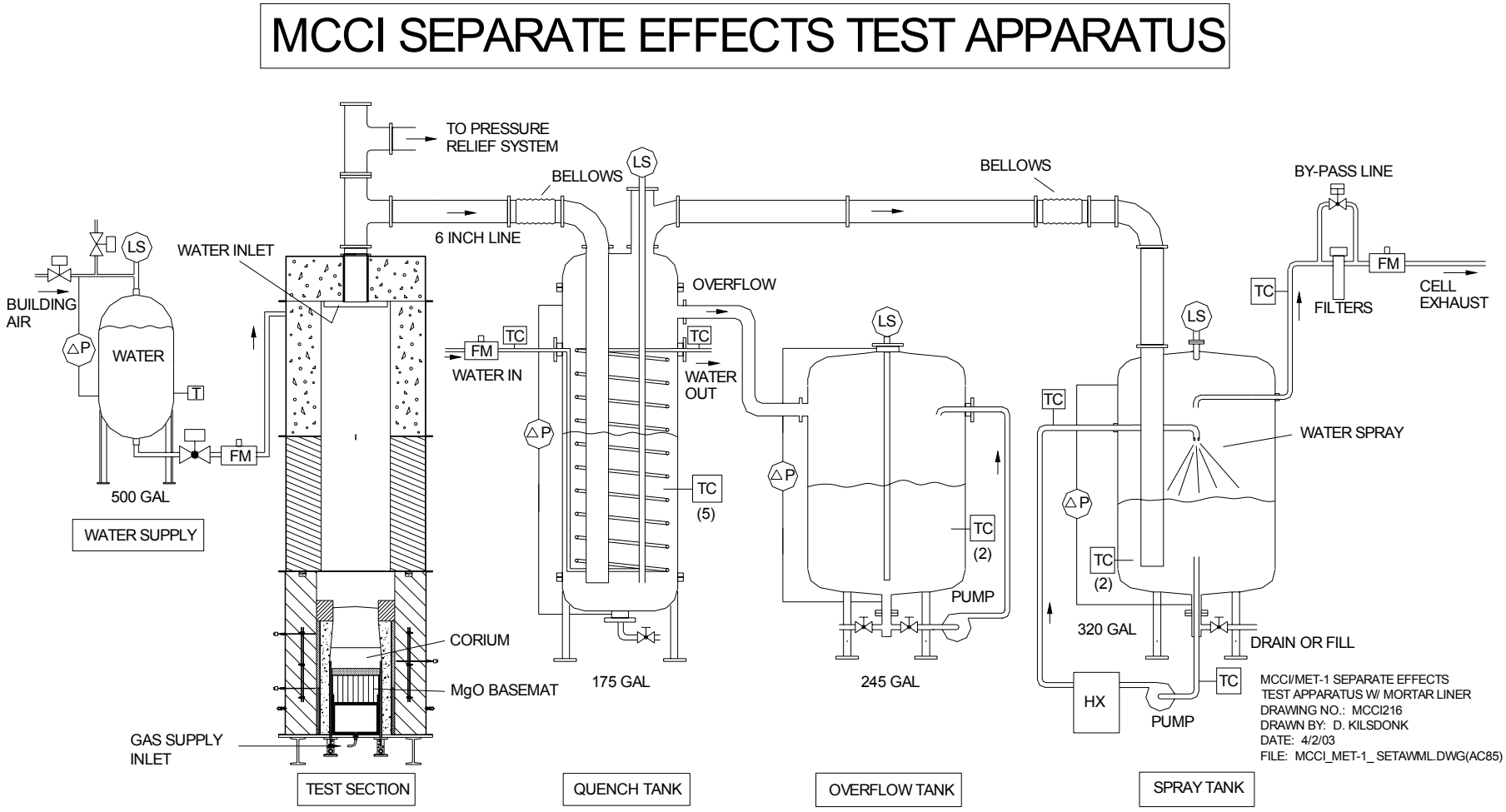

Figure 2.1. Basic Elements of the MET Apparatus.

With the exception of the mortar liner, these modifications are noted to be identical to those used in the first MACE Separate Effects Test.

The test section for containment of the corium melt is 3.4 m tall with a square internal cross-section. The porous MgO basemat is located at the bottom of the test section. The original 50 cm x 50 cm lower section design[1] is shown in Figure 2.2 for reference, while the revised section incorporating the mortar liner is shown in Figure 2.3. As is evident from comparing the two figures, the UO_2 pellet liner with back-up refractory MgO sidewalls are maintained in the revised section, with the mortar sidewalls installed within the pellet liner. This approach has the advantage of maintaining the inert sidewall design as the ultimate barrier precluding sidewall melt-through (which is a Safety Plan requirement), while incorporating the mortar liner within the boundaries of the existing test section. The mortar liner will obviously undergo ablation during the test. From a scaling viewpoint, this approach has the disadvantage of reducing the effective cross-sectional area of the test section from 50 cm x 50 cm to 37.5 cm x 37.5 cm (i.e., 44% area reduction). However, if the mortar liner is successful in precluding crust attachment to the test section sidewalls, then prototypic crust formation behavior should be observed in the smaller cross section.

As shown in Figure 2.3, the exothermic chemical mixture used to generate the melt is placed on top of the porous basemat. The thermite reaction is initiated by tungsten starter coils located near the top of the powder charge. Once the chemical reaction is complete (~ 30 seconds), a 560 kW AC power supply is used to apply Direct Electrical Heating (DEH) to the melt through two banks of tungsten electrodes located on opposite sidewalls of the test section. The overall heating rate is adjusted to correspond to a specified decay heat level for the experiment (nominally 300 W/kg fuel). Note from Figure 2.3 that the tungsten electrode height in the revised design has been reduced to well below the initial collapsed melt height, so that the crust is not able to mechanically bond to the electrodes during the test. Although the electrical current density in the melt is not uniform due to the elevation reduction, experience in the MACE program has shown that mixing associated with gas sparging is sufficient to uniformly distribute the corresponding energy input across the extent of the melt.

The inert basemat is constructed from castable MgO. The basemat is 18 cm thick, and is cast with an array of 1.0 mm diameter holes with a surface density of 7 holes/100 cm^2. This hole density is slightly coarser than that used by Brockmann et al.[3] in their void fraction study using molten stainless steel. The holes are produced by casting an array of steel wires into the basemat. The wires are removed after casting and curing at 280 C. As shown in Figure 2.3, the upper surface of the MgO is also protected by a 5 cm thick layer of crushed UO_2 pellets that serves two purposes: i) prevent freezing-induced plugging of the holes after the melt generation phase, and ii) enhance the uniformity of the gas flow through the melt by acting as a secondary sparger plate. During the melt generation phase, a slow gas purge through the basemat ensures that a uniform flow field is established and maintained. The basemat design shown in Figure 2.3 is essentially the same as that employed in the first MACE melt eruption test, except that the MgO thickness has been increased (from 15 to 18 cm), and the thickness of the protective UO_2 pellet layer has been increased (from 2.5 to 5 cm). Both of these measures are intended to increase the resistance of the basemat to attack by the corium melt.

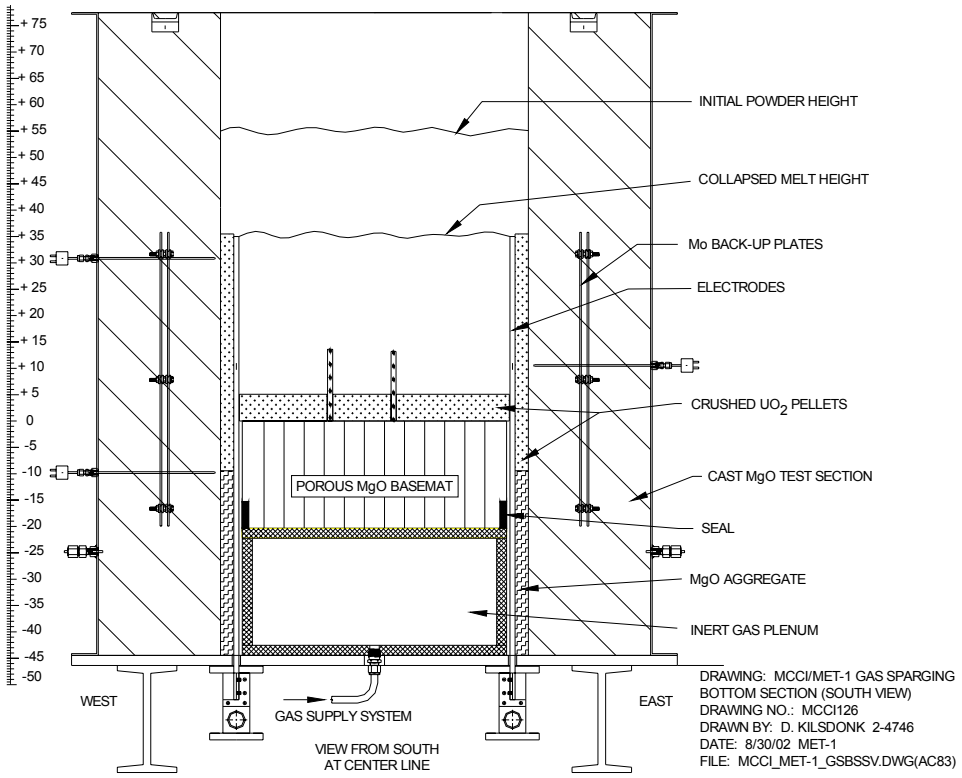

Figure 2.2. Details of the Original[1] MET Lower Test Section Design.

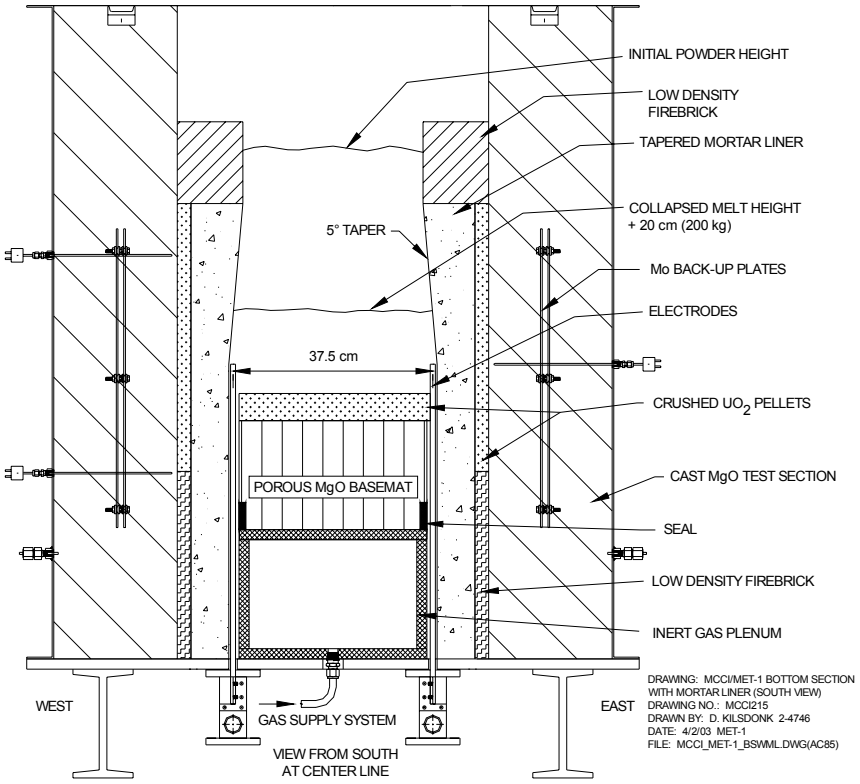

Figure 2.3. Revised MET Lower Section Design With Mortar Liner.

The configuration of the basemat gas supply system is shown in Figures 2.4 and 2.5. The gas used to mock up the basemat decomposition gases is a specialty blend of argon and helium, with the relative ratio of these two gases selected such that the mixture density is the same as the decomposition gas for a given type of concrete. The primary side of the gas supply system consists of a parallel bank of critical flow orifices to provide preset, incremental flow rates to the test section. The use of critical flow orifices is obviously advantageous since the flow rate is fairly insensitive to downstream pressure conditions. The backup side of the flow control system consists of a Hastings mass flow controller with continuous flow rate adjustment capability (0-1000 slpm); the controller electronics are wired into the control room so that the flow rate can be remotely adjusted during the test.

Water is delivered above the melt by two weirs located at the top of the test section on the sidewalls adjacent to those with the electrodes. Water can be supplied over a wide range of flow rates. In previous MACE tests, the water was initially added at a steady rate to ensure that the quench process was not water-starved (i.e., sufficient to sustain a quench rate of at least 10 MW/m^2) until a 50 cm head is established. Thereafter, makeup was added to maintain the head in the range of 50 +/- 5 cm as the quench process continues.

A 15 cm diameter gas line on the lid of the test section vents steam and noncondensables to the adjacent primary quench tank, which is cooled with a large coil. An overflow tank collects excess condensate from the quench tank. Downstream from the quench tank is a secondary spray tank that performs an identical condensation/gas cleanup function. While adding redundancy, the use of two tanks in series overcomes the practical limitation of attempting to resolve melt/water heat fluxes from as high as 5 MW/m^2 during the initial bulk cooling stage to as low as a few hundred kW/m^2 depending on upper crust behavior.

After passing through the quench system, the inert basemat gas and any noncondensables arising from the melt/water interaction are vented through an off gas system that includes a demister, filters, and gas flow meter. The off gases are eventually exhausted through the containment cell ventilation system where it flows through a series of high efficiency filters before finally being released from the building stack.

2.2 Instrumentation

Instrumentation is selected to provide the necessary measurements to determine the time dependent melt/water heat flux and the melt temperature distribution. In terms of evaluating the melt/water heat flux, the water supply tank is equipped with level sensors and a flow meter to measure the water addition rate to the test section. The test section is equipped with water level sensors, thermocouples, and pressure transducers to monitor the water level over the melt, and correct the steaming rate for quenching of extraneous structures above the melt surface. The quench system tanks are instrumented with thermocouples, level sensors, and pressure transducers to monitor transient energy deposition in the system so that the necessary energy balance information can be extracted.

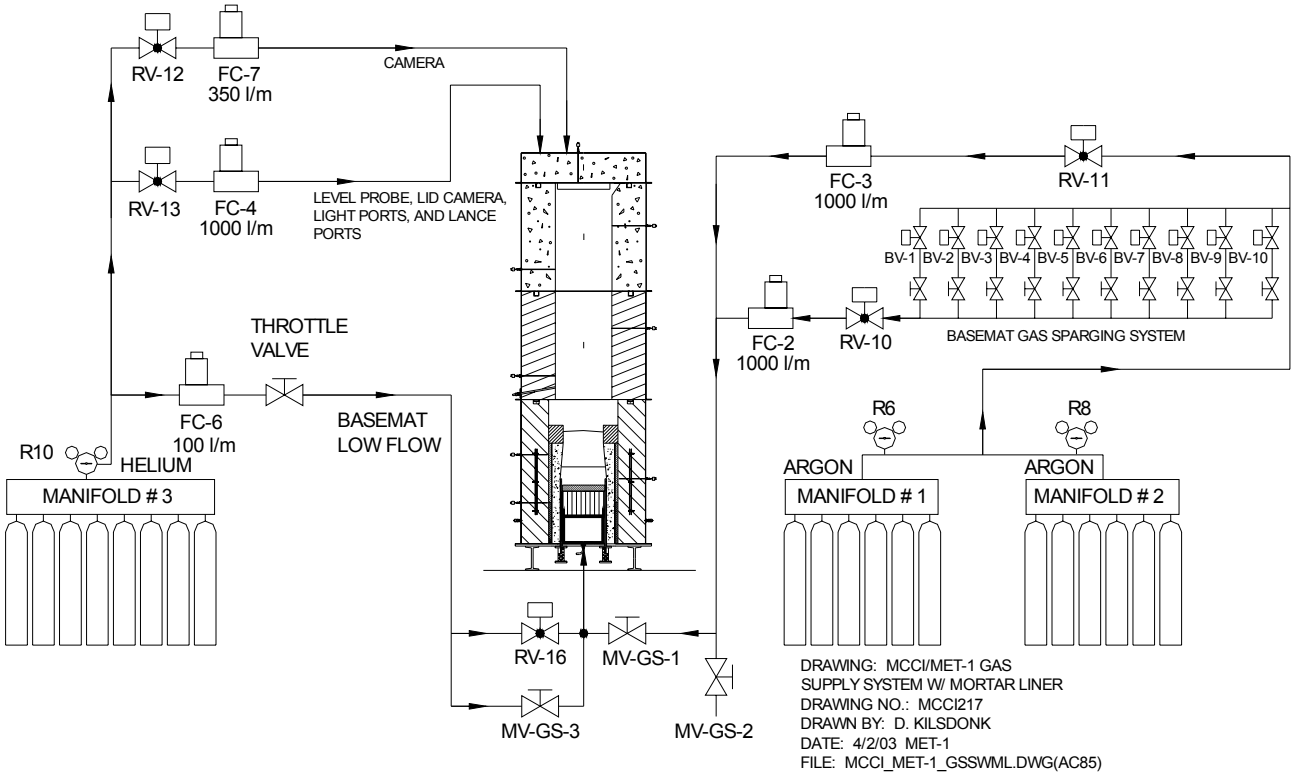

Figure 2.4. Overview of the MET Gas Supply System.

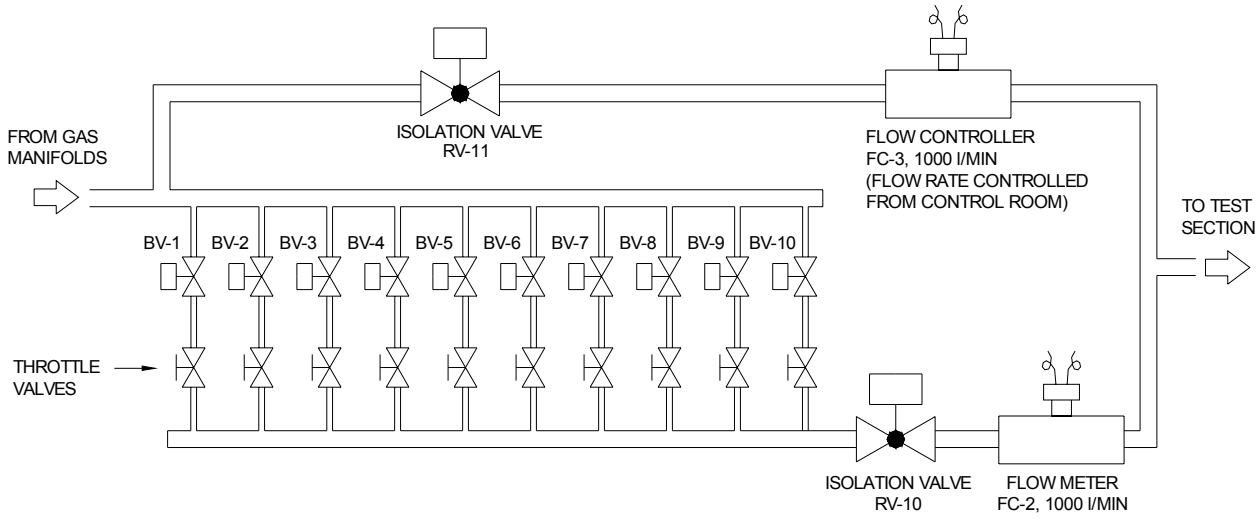

VALVE NUMBER	BV-1	BV-2	BV-3	BV-4	BV-5	BV-6	BV-7	BV-8	BV-9
FLOW RATE (SLPM/VALVE)	25	25	25	25	25	25	25	25	25
TOTAL FLOW RATE (SLPM)	25	50	75	100	125	150	175	200	225
CORRESPONDING MELT SPARGING RATE AT 2000K (50 cm X 50 cm)	2.5	5.0	7.5	10.0	12.5	15.0	17.5	20.0	22.5

DRAWING: MCCI/MET-1 BASEMAT GAS SPARGING SYSTEM W/ MORTAR LINER
DRAWING NO.: MCCI218
DRAWN BY: D. KILSDONK
DATE: 4/2/03 MET-1
FILE: MCCI_MET-1_BGSSWML.DWG(AC85)

Figure 2.5. Details of the MET Basemat Gas Supply System.

A plan view of the basemat instrumentation layout is provided in Figure 2.6, while an elevation view of the Type C melt temperature thermocouple locations is shown in Figure 2.7. As is evident from these figures, a total of five three-junction Type C thermocouple assemblies within tungsten thermowells are provided to measure melt temperature. Consistent with the approach of trying to maintain a floating crust boundary condition, these assemblies are kept low within the pool (i.e., elevations $\leq$ melt axial centerline) so that they will not inhibit downward crust relocation. The basemat is also cast with a total of three four-junction Type K thermocouple assemblies embedded within the basemat. These arrays are provided to monitor the basemat temperature during the test. The information from these TC's will be used to evaluate the heat loss into the underlying MgO using standard inverse heat conduction techniques.

Other significant test instrumentation includes both stationary (lid mounted) and insertable (water cooled) video cameras for observing various stages of the melt/water interaction. Several fast response, high range (piezo-electric) pressure transducers are mounted at various locations within the test section to capture the pressure pulse due to a steam explosion, should one occur.

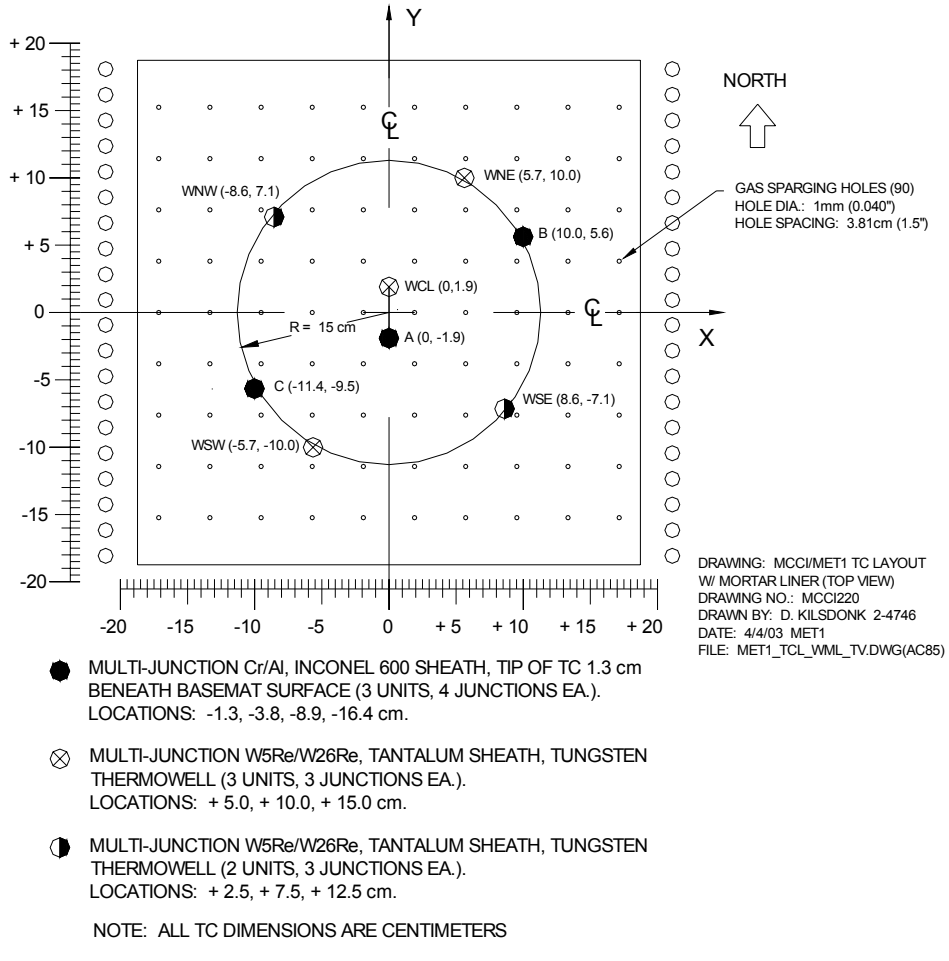

Figure 2.6. Plan View of the MET MgO Basemat Instrumentation Layout.

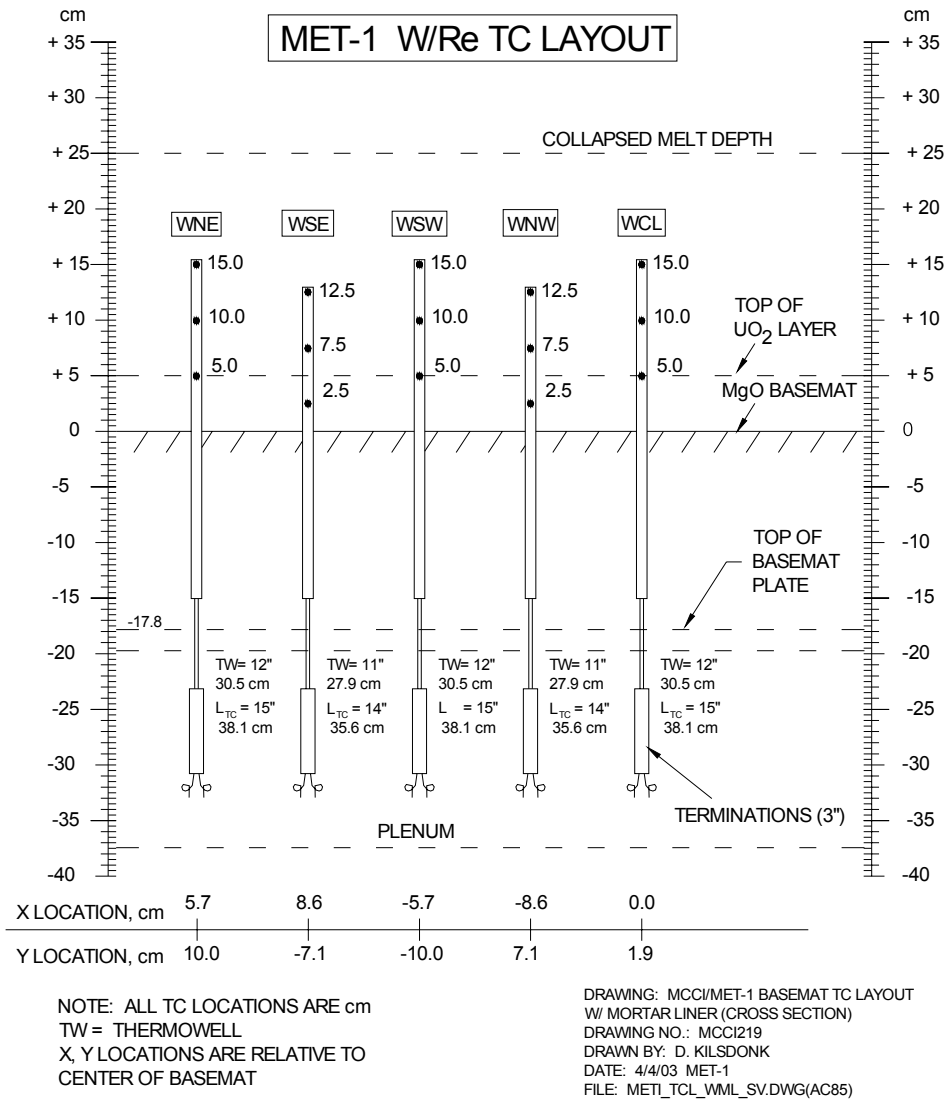

Figure 2.7. Elevation View of Type C Thermocouple Junction Locations.

2.3 Data Acquisition and Control Systems

All data acquisition and process control tasks are managed by a PC executing LabVIEW 6.i under Windows XP. Sensor output terminals are connected to model HP E1345A 16-channel multiplexers and the signals are digitized by an HP E1326B 5 ½ digit multimeter located within the test cell; see Figure 2.8. Signal noise is reduced by integration over a single power line cycle (16.7 ms). The digitized sensor readings are routed from the test cell to the PC in the control room via two HP-IB extenders. The extenders allow the ASCII data from the HP to be sent through the cell wall over a BNC cable. The extender within the control room then communicates with a GPIB card within the PC. This configuration also permits remote control of the multimeter through LabVIEW. The power line cycle integration results in a minimum (theoretical) time of ~ 3.3 s to scan the channel list (16.7 ms • 200 channels). In practice, however, the acquisition of a single scan is at a frequency of approximately 0.2 Hz.

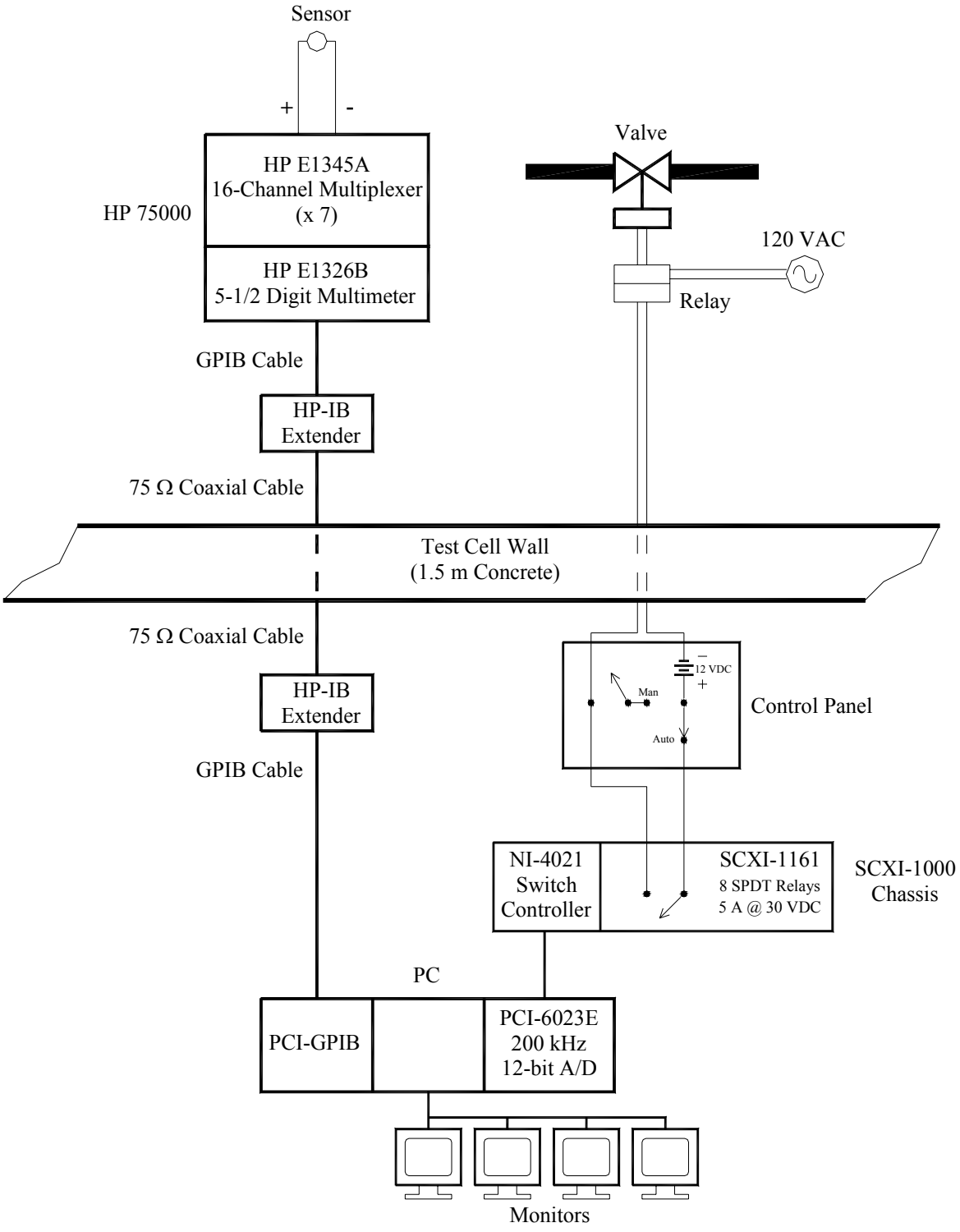

Figure 2.8. MET Data Acquisition and Control Systems.

Valves are controlled with the PC using a relay card housed within an SCXI chassis (National Instruments). These electromechanical relays are capable of switching up to 8 A at 125 VAC or 5 A at 30 VDC. They are operated via a switch controller in the SCXI chassis, which communicates with the PC through a general-purpose data acquisition card. As shown in Figure 2.8, the relays in the control room operate devices within the test cell indirectly, through a second relay. This is intended to provide an additional level of electrical isolation between the NI switching hardware and high voltage sources within the cell. As an added safety measure, all wiring is routed through a control panel that can be switched from automatic (PC) control to manual control in the event of computer failure. The system is currently configured to operate eight relays, but expansion to 24 is possible.

2.4 Corium Composition

For the first test with this apparatus, it is recommended to utilize a fully oxidized (with respect to cladding oxidation) corium melt containing nominally 8 wt % siliceous concrete decomposition products. The first melt eruption separate effects test was conducted in the MACE program with a corium melt containing ~ 8 wt % limestone/common sand concrete decomposition products. Thus, the use of corium containing siliceous concrete will serve to augment the existing database. Although adjustments are possible, it is recommended to conduct the first test with an initial melt pool depth of 20 cm; the corresponding melt mass is ~200 kg. The thermite reaction that produces the target melt composition is of the form:

$$1.22U_3O_8 + 3.3Zr + 0.58Si + 1.14SiO_2 + 0.026Mg + 0.36\,CaO + 0.12Al + 1.842CrO_3 \rightarrow$$

$$3.66UO_2 + 3.3ZrO_2 + 1.72SiO_2 + 0.026MgO + 0.91CaO + 0.36Al_2O_3 + 1.842Cr;$$

$$Q = -252.2 \text{ kJ/mole } (1.71 \text{ MJ/kg});$$

$$T_{adiabatic} = 2570\ ^{\circ}C;\ T_{actual} \sim 2200\ ^{\circ}C$$

The composition of the melt produced from this reaction is summarized in Table 2.1, while the detailed pre- and post-reaction compositions are provided in Table 2.2. This thermite composition is essentially the same as that employed in the SSWICS-2 experiment, which was a dedicated separate effects test investigating the water ingression cooling mechanism with a corium composition containing 8 wt % siliceous concrete as an initial constituent.

Table 2.1. Initial Melt Composition for MET-1.

Constituent	Wt%
UO_2	60.97
ZrO_2	25.04
Calcined Concrete	8.08[a]
Cr	5.91

[a]Calcined siliceous concrete, consisting of 79.0/0.9/15.4/4.7 wt% SiO_2/MgO/CaO/Al_2O_3

Table 2.2. Detailed Pre- and Post-Reaction Compositions for MET-1 Thermite.

Constituent	Wt %	
	Reactant	Product
U_3O_8	63.38	-
UO_2	-	60.97
Zr	18.53	-
ZrO_2	-	25.04
Si	1.00	-
SiO_2	4.23	6.38
Mg	0.04	-
MgO	-	0.07
Al	0.20	-
Al_2O_3	-	0.38
CaO	1.25	1.25
CrO_3	11.37	-
Cr	-	5.91

3.0 TEST OPERATING PROCEDURE

Based on the above discussions, test specifications for MET-1 are summarized in Table 3.1. The initial target decay heat level, simulated by Direct Electrical Heating (DEH), is tentatively specified as 300 W/kg UO_2. This corresponds to a gross input power of 37 kW for the 121.9 kg UO_2 present in the 200 kg corium inventory (see Table 2.1). Since the sidewalls of the apparatus are constructed from mortar and are expected to undergo ablation, no correction for sidewall energy deposition is proposed. An overall strategy for operating the power supply and the basemat gas sparging system is presented below. The strategy is intended to allow the melt eruption and water ingression cooling mechanisms to develop and progress in as natural a manner as possible given the experimental limitations. The procedure can obviously be modified according to input from the PRG. This strategy is summarized as follows:

1) Establish a helium gas flow of 50 slpm through the basemat to preclude hole plugging when the burn front reaches the bottom of the test section.

2) Ignite the thermite by applying 60 Amps to each of the four tungsten starter coils located at the top of the charge. Once the burn is complete (~ 1 minute), adjust the system parameters as follows in preparation for flooding of the cavity:

   a) Start the basemat gas system with the specialty gas mixture at a rate of 60 slpm (~ 3 cm/sec sparging rate), and then terminate He flow to the basemat.

   b) Ramp the power supply at a rate of ~ 3000 Amps/minute up to an initial preheat level of 100 kW (do not exceed maximum current limit of 9200 Amps). Once target power (or current limit) is reached, maintain constant power operation until the melt temperature climbs to the initial target level of 2200 ˚C, or it stabilizes for a period of 10 minutes at a lower level.

3) The criteria for flooding the cavity are: i) the melt temperature is raised to 2200 ˚C, or ii) thermal equilibrium has been achieved at a lower value. Once the criteria are met, bring the input power to the initial target of 37 kW and hold for two minutes. After the two-minute hold, flood the cavity to a collapsed water height of 50 cm over the melt surface.

4) After the cavity is flooded, maintain input power constant at the 37 kW level during the initial bulk cooling phase until incipient crust formation occurs. Completion of bulk cooling will be characterized by the following: i) melt temperature passes through a valley and then starts to increase, and ii) power supply voltage at constant input power goes through a plateau and then starts to decrease. Once these markers are observed, record DAS time, and begin insertion of underwater video camera.

5) After incipient crust formation, begin power supply operation in constant specific power mode and maintain power density in the melt zone in the range of 300 +50/-0% W/kg fuel for the balance of the test. (The power density in the melt zone is calculated on-line using the corium resistivity correlation developed in the MACE program.)

Table 3.1. Summary of Test Specifications for MET-1.

Parameter	Specification
Corium Composition	100 % Oxidized, 8 wt % Siliceous Concrete
Corium Mass	200 kg
Basemat Type	Porous Inert (MgO) With Remotely Controlled Gas Sparging
Sidewall Type	Mortar
Basemat Cross-Sectional Area	37.5 cm x 37.5 cm
Initial Melt Depth	20 cm
Initial Melt Temperature	2200 ˚C
System Pressure	1 atmosphere (nominal)
Criteria for Water Addition	Melt Temperature Stabilizes at 2200 ˚C or Maximum Achievable
Initial/Makeup Water Flow Rates (equivalent to 20 MW/m^2 quench rate)	2 l/sec
Sustained Collapsed Water Level (Volume)	50 cm ± 5 cm (125 l ± 13 l)
Inlet Water Temperature	296 K
Power Supply Operating Mode After Water Addition	Constant Specific Power Density in Melt Zone of ~ 300 W/kg UO_2
Test Termination Criteria	(1) Corium is Quenched, or (2) Steady State Conditions are Reached at Max. Sparging Rate

6) Maintain a constant basemat gas flow rate at the initial level of 3 cm/sec until steady state conditions are achieved with no coolability mechanisms active for a

period of 10 minutes (i.e., eruptions are not evident on the video cameras, and steady state power supply operating conditions have been achieved).

7) After steady state conditions are achieved, increase the superficial gas velocity by an increment of 3 cm/sec.

8) Repeat Steps 6 and 7 until either steady-state conditions have been achieved at the peak gas flow rate or the debris has quenched.

9) Terminate the test.

The peak gas flow rate referred to in Step 8 of the procedure can be specified at any desired level. A preliminary ceiling of 12 cm/sec is set for the purposes of discussion. The mass of corium ejected during each constant flowrate interval is determined by the integrated energy deposition in the quench system, in conjunction with the change in specific enthalpy during quench of the ejected material from the melt temperature down to the water saturation temperature (this same approach was used to assess the ejected melt mass in the MACE melt eruption separate effects test). In this manner, a plot of corium entrainment rate as a function of sparging rate can be produced. The corium entrainment coefficient, which is the essential piece of information to be gained from this test, is the slope of the line in this graph.

During the experiment sequence, both the lid and submersible video cameras would be used to observe the eruptions, with the primary objective of discriminating between periods of particle ejections versus single phase extrusions (i.e., lava flow) events. This visual information, in conjunction with the estimated time-dependent particle bed mass/depth evaluated by the above described method, is intended to support model development activities. In particular, the visual information will allow the correlation of the entrainment rate with the physical characteristics of the ejection process, while factoring in the depth of debris through which the process is occurring.

4.0 SCOPING TEST FOR EVALUATION OF MORTAR LINER APPROACH

As described in Section 1.0, the PRG recommended the development of a conceptual design for a small-scale scoping test to verify the ability of the mortar liner to preclude formation of an anchored bridge crust under core-concrete interaction conditions. The purpose of this section is to provide this design for PRG review. The overall approach is to conduct a transient quench experiment in which a thermite reaction is used to produce a corium melt in a mortar crucible with tapered sidewalls (i.e., with the same basic design elements planned for the full scale test; see Section 2.0). An illustration of the test crucible is shown in Figure 4.1. As is evident from the figure, the crucible is cylindrical, with the same 5° sidewall taper used in the full scale test (see Figure 2.3). The average crucible diameter near the melt centerline is 18 cm. The initial collapsed melt depth for the test is proposed to be 12.5 cm. Thus, this test will utilize an initial corium mass of nominally 17 kg to provide the required melt volume of 3.2 liters.

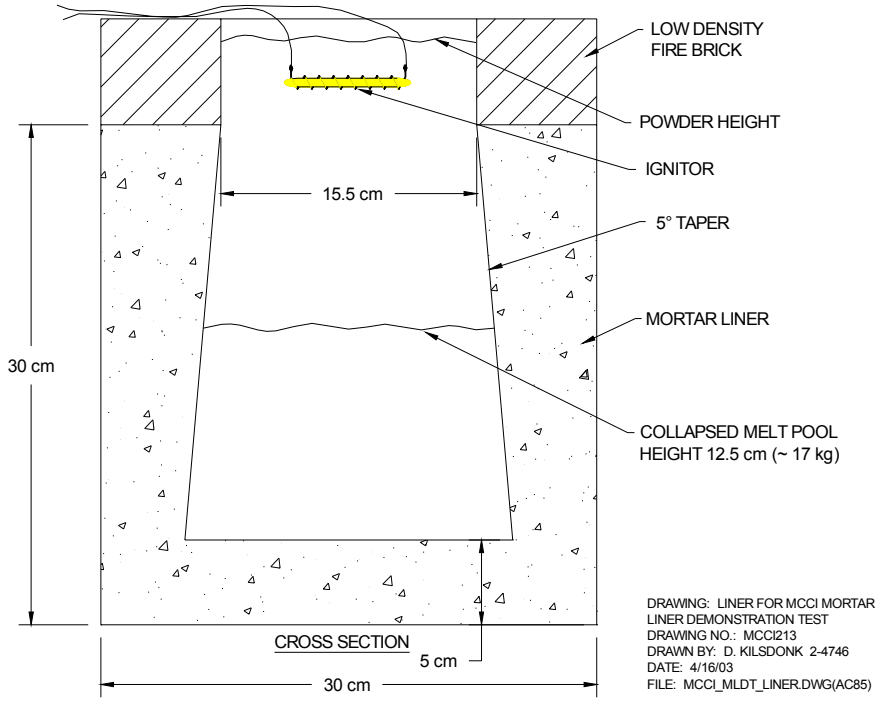

Figure 4.1. Crucible Design for Mortar Liner Scoping Test.

As discussed later in this section, the thermite is designed to achieve a relatively high reaction temperature of ~ 2300 °C, so that the sensible energy within the melt is sufficient to initiate core-concrete interaction. After the interaction begins, the melt will be flooded with water from above. The interaction will be allowed to continue until the corium is completely quenched. In order to provide a metered flow rate of water during the quench phase, and also to condense the steam from the interaction in an instrumented system for evaluation of the melt/water heat flux, the test crucible is designed to fit within the SSWICS test vessel,[4] as shown in Figure 4.2. It is proposed to carry out this experiment at atmospheric pressure. Prior to initiating the thermite reaction, the entire test vessel and interconnected piping will be heated to 100 °C (viz. saturation temperature at atmospheric pressure) using existing SSWICS test equipment. As a result, the melt/water heat flux evaluated from the test data should be quite accurate, since structure heat sink effects will be minimal. Note from Figure 4.2 that a single Type C thermocouple is introduced from the bottom of the crucible to provide a measurement of the initial melt temperature, and also to indicate when the thermite reaction is complete.

As stated above, the thermite is designed to produce a high reaction temperature so that core-concrete interaction conditions can be achieved based on the sensible energy content of the melt. The particular reaction proposed for this experiment is as follows:

$$0.097U_3O_8 + 0.23Zr + 0.351Si + 0.034Al + 0.0289MgO + 0.125CaO + 0.34CrO_3 \rightarrow$$

$$0.291UO_2 + 0.23ZrO_2 + 0.351SiO_2 + 0.017Al_2O_3 + 0.0289MgO + 0.125CaO + 0.34Cr;$$

$$Q = -254.9 \text{ kJ/mole } (2.28 \text{ MJ/kg});$$

$$T_{adiabatic} = 2680 \text{ °C}, T_{actual} \sim 2300 \text{ °C}$$

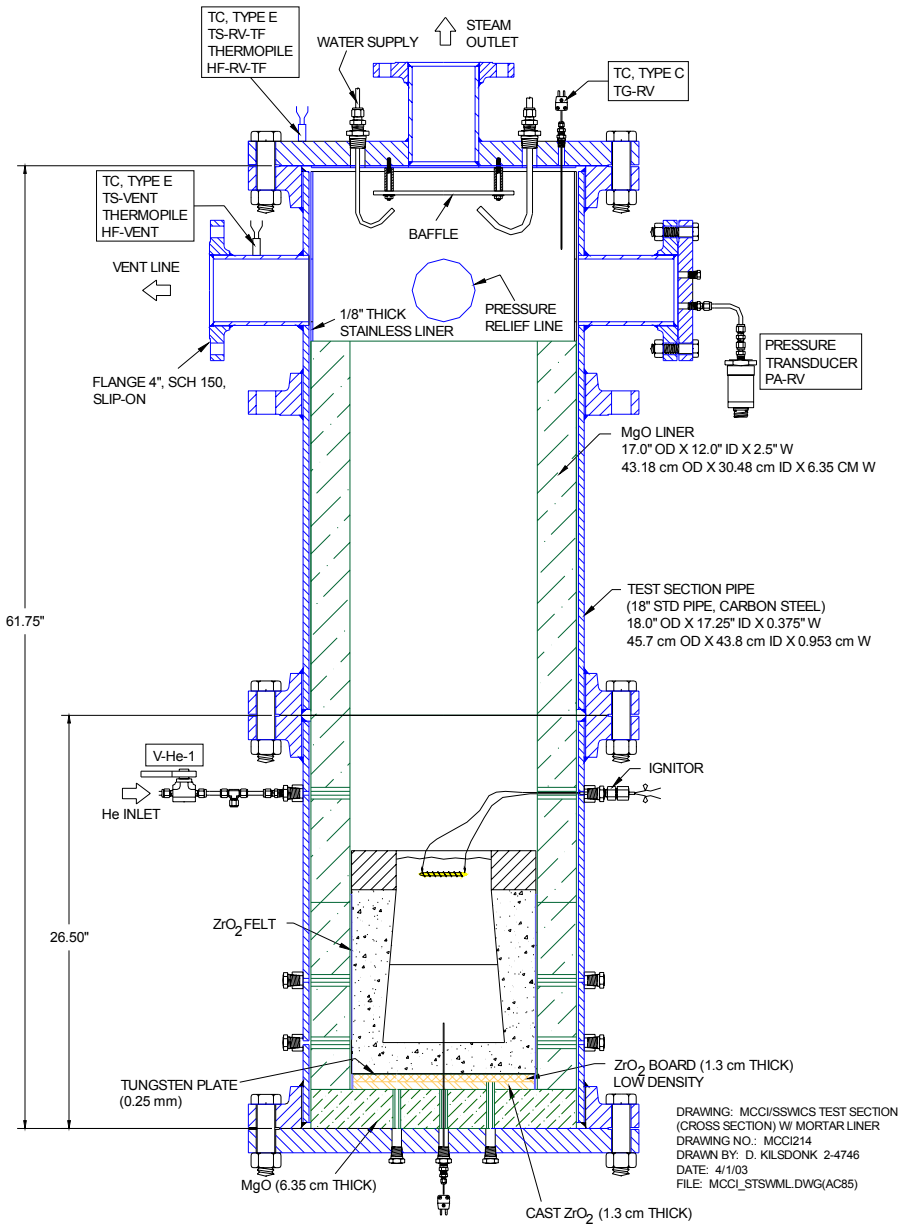

Figure 4.2. Test Crucible Installed within SSWICS Reaction Vessel.

The overall composition of the melt produced from this reaction is summarized in Table 4.1, while the detailed pre- and post-reaction compositions are provided in Table 4.2. Examination of Table 4.1 indicates that the post-reaction composition closely approximates a fully oxidized PWR core containing ~ 20 wt % high silica concrete decomposition byproducts. This thermite composition is very similar to that used in the COMET-2 debris coolability experiment.[5] (The only notable exception is that the 1.27 wt % B_2O_3 present in the initial thermite mixture has been omitted). In that test, the melt rapidly eroded through several centimeters of high silica concrete following completion of the thermite reaction. Thus, this mixture is expected to produce the desired core-concrete interaction conditions for evaluating the ability of the mortar liner to preclude stable bridge crust formation during corium quench.

After the experiment, the crucible will be removed from the test vessel and vertically sectioned along the axial centerline to reveal the axial debris distribution. Insofar as the mortar liner concept is concerned, the success criteria is that the corium undergoes cool down and solidification from core-concrete interaction conditions without the formation of a voided region that separates the crust from the underlying corium ingot.

Table 4.1. Proposed Melt Composition for Mortar Liner Scoping Test.

Constituent	Wt%
UO_2	50.57
ZrO_2	18.18
Calcined Concrete	19.90[a]
Cr	11.35

[a]High silica concrete, consisting of 68.0/22.6/3.8/5.6 wt% SiO_2/CaO/MgO /Al_2O_3

Table 4.2. Detailed Pre- and Post-Reaction Compositions for Proposed Thermite.

.Constituent	Wt %	
	Reactant	**Product**
U_3O_8	52.53	-
UO_2	-	50.57
Zr	13.45	-
ZrO_2	-	18.18
Si	6.34	-
SiO_2	-	13.54
MgO	0.74	0.74
Al	0.60	-
Al_2O_3	-	1.12
CaO	4.50	4.50
CrO_3	21.84	-
Cr	-	11.35

5.0 REFERENCES

1. M. T. Farmer, S. Lomperski, D. J. Kilsdonk, and R. W. Aeschlimann, "Melt Eruption Test (MET) Design Report," OECD/MCCI-2002-TR03, Rev. 0, September 19, 2002.

2. M. T. Farmer, B. W. Spencer, D. J. Kilsdonk, and R. W. Aeschlimann, "Results of MACE Corium Coolability Experiments M0 and M1b," Proc. 8th Int. Conf. on Nucl. Eng., ICONE-8175, April 2-6, 2000.

3. J. E. Brockmann, R. E. Arellano, and D. A. Lucero, "Validation of Models of Gas Holdup in the CORCON Code," NUREG/CR-5433, SAND89-1951, December, 1989.

4. M. T. Farmer, S. Lomperski, D. J. Kilsdonk, R. W. Aeschlimann, and P. Pfeiffer, "Small-Scale Water Ingression and Crust Strength Tests (SSWICS) Design Report," Rev. 1, OECD/MCCI-2002-TR01, September 20, 2002.

5. H. Alsmeyer, M. T. Farmer et al., "The COMET-Concept for Cooling of Ex-Vessel Corium Melts," 6th Int. Conf. on Nucl. Eng., ICONE-6086, May 10-14, 1998.